PHYSICAL REVIEW C **94**, 054312 (2016)

High spin γ-ray spectroscopy in ^{41}Ca

R. Bhattacharjee, S. Samanta, S. Das, S. S. Bhattacharjee,[*] R. Raut,[†] and S. S. Ghugre
UGC-DAE Consortium for Scientific Research, Kolkata Centre, Kolkata 700098, India

A. K. Sinha
UGC-DAE Consortium for Scientific Research, Indore Centre, University Campus, Khandwa Road, Indore 452017, India

U. Garg
Department of Physics, University of Notre Dame, Notre Dame, Indiana 46556, USA

R. Chakrabarti
K. J. Somaiya College of Science and Commerce, Vidyavihar, Mumbai 400077, India

S. Mukhopadhyay
Nuclear Physics Division, Bhabha Atomic Research Centre, Mumbai 400085, India

A. Dhal, R. P. Singh, N. Madhavan, and S. Muralithar
Inter University Accelerator Centre, Aruna Asaf Ali Marg, New Delhi 110067, India
(Received 19 July 2016; published 14 November 2016)

High spin states in ^{41}Ca have been investigated by using γ-ray spectroscopic techniques following the ^{27}Al(^{16}O$\,,pn)^{41}$Ca fusion-evaporation reaction. Around twelve new transitions belonging to ^{41}Ca have been observed and placed in the level scheme, which now has been extended up to $E_x \sim 9$ MeV. The spin-parity assignments for the observed levels were arrived at following the analysis of both the coincidence intensity anisotropies and linear polarization measurements. The established 5p-4h band was extended up to $J^\pi = 19/2^-$. The observations of Doppler shape and shifts facilitated the estimation of the level lifetimes by using the Doppler shift attenuation method. The lifetimes were validated with respect to previous measurements and lifetime of a few levels has been arrived at for the first time. Shell-model calculations were carried out to explain the observed level structure of the nucleus and are indicative of both single-particle and collective degrees of freedom in this $N \sim Z \sim 20$ nucleus.

DOI: 10.1103/PhysRevC.94.054312

I. INTRODUCTION

The structure of the nuclei in the light-mass region ($A \sim 30$–40) is complicated due to the competition and/or coexistence between single-particle and collective excitations. Interestingly, even near the double shell closure $N \sim Z \sim 20$, the core excitation may compete energetically with the single-particle excitations. The structure of several odd-A nuclei with $A \sim 40$, which have nucleons in the lower part of the $1f_{7/2}$ shell, has provided evidence for nucleon excitations from the ^{40}Ca core across the sd-fp shell gap [1]. Evidence has also been established for the dominance of multiparticle excitations in this region that favors the onset of deformation [moderate to substantial]. Thus, the structure of these nuclei may reveal intriguing features based on the interplay of the single and collective degrees of freedom.

The ^{41}Ca nucleus with a single nucleon outside the ^{40}Ca core might be considered as one of the simplest cases to investigate the aforementioned features. However, the level structure of the nucleus, as revealed from the previous studies, was noted to be more obscure than expected from a single valence nucleon outside the double magic (^{40}Ca) core and was attributed to the interplay of the single particle and core excited configuration [2]. Several theoretical efforts, including shell-model calculations using restricted ($d_{3/2}f_{7/2}$) as well as extended ($2s_{1/2}1d_{3/2}1f_{7/2}2p_{1/2}$) model space, were dedicated to interpret these excitations. Such endeavors notwithstanding, the experimental data on the nucleus are still too sparse to constrain and/or refine the theory. Earlier measurements [2–5] of the nucleus have established the level structure up to an excitation energy of ~7 MeV. These measurements, essentially dated more than three decades back, were carried out in limited scope and using modest experimental setups. Apart from the limited spectroscopic information acquired in these studies, the results obtained therefrom were often with considerable uncertainties and, at times, discrepant. For instance, linear polarization measurements for several $A \sim 40$ nuclei were reported by Olness *et al.* [6] wherein the 1608 keV ($19/2^-_1 \rightarrow 17/2^+_1$) transition in ^{41}Ca, which is known to be electric in nature [4] and expected to have a positive polarization (P), was reported to have $P = -0.26 \pm 0.34$.

In this light, the present work reports a reexamination of the level structure of ^{41}Ca by using a heavy-ion-induced

---

[*] Present Address: Inter University Accelerator Centre, Aruna Asaf Ali Marg, New Delhi 110067, India.

[†] rraut@alpha.iuc.res.in

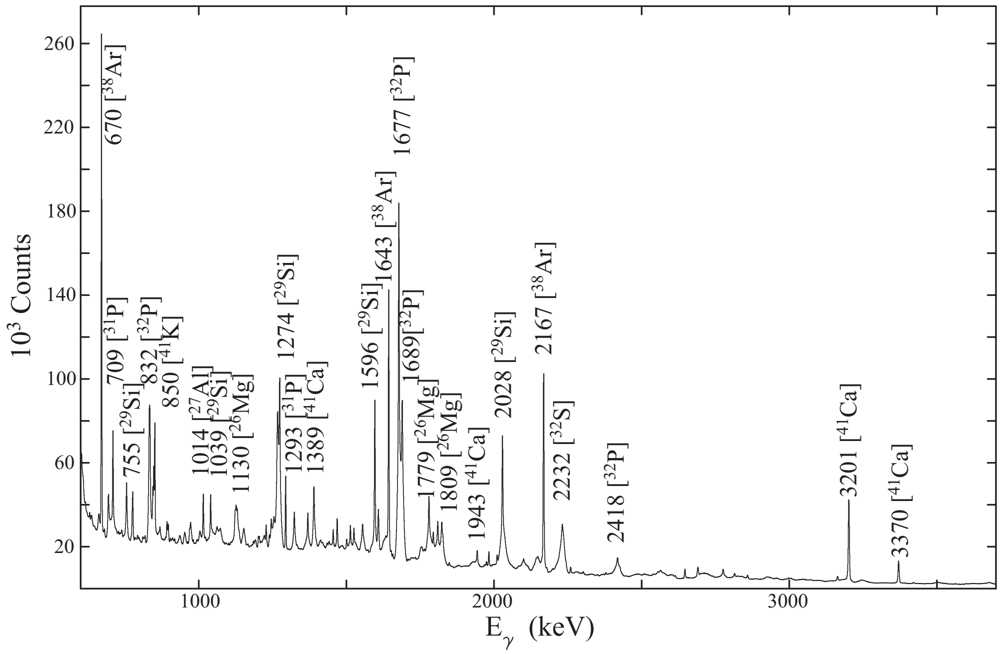

FIG. 1. Projection spectrum of ^{16}O + ^{27}Al reaction at an incident beam energy of 34 MeV. Nuclei in the $A \sim 30$ region were populated from the reaction of ^{16}O beam with the Ta_2O_5 target (please see text for details).

fusion-evaporation reaction to populate the nucleus of interest and high-resolution γ-ray spectroscopy tools. Shell-model calculations have also been carried out and the results have been compared with the measurements.

II. EXPERIMENTAL DETAILS AND DATA ANALYSIS

In the present work, the excited states of the ^{41}Ca nucleus were populated by using the ^{27}Al(^{16}O , pn) fusion-evaporation reaction at $E_{\text{lab}} = 34$ MeV. The ^{16}O beam was provided by the 15 UD Pelletron Accelerator facility at the Inter University Accelerator Centre (IUAC), New Delhi. The target was a thick piece of mono-isotopic natural aluminum. Actually, the present data resulted from an experiment wherein the target frame was of aluminum. The experiment originally pertained to the spectroscopy of *sdpf* nuclei in the $A \sim 30$ region and used ^{18}O, in the form of Ta_2O_5, as the target. However, a part of the beam hit the aluminum target frame and populated nuclei in the $A \sim 40$ region, some of which, ^{41}Ca for instance, had sufficient statistics for independent spectroscopic investigation. Deexciting γ rays were detected by using the Indian National Gamma Array (INGA) [7], then comprising of 18 Compton-suppressed Clover detectors. The detectors were placed at angles $\theta = 32^\circ$ (three detectors), 57° (four detectors), 90° (five detectors), 123° (three detectors), and 148° (three detectors) with respect to the beam direction. The pulse processing was carried out by using the Clover electronics modules, each supporting one Compton suppressed Clover detector, designed and fabricated [8] at IUAC, New Delhi. The data-acquisition system was CAMAC based and supported by the CANDLE software [9]. The trigger condition for the acquisition was set at a minimum Clover multiplicity of two. Energy calibration was performed by using the radioactive sources ^{152}Eu, ^{133}Ba, and ^{60}Co along with the beam-off radioactivity data. The data were subsequently sorted into the symmetric and asymmetric (angle-dependent) E_γ-E_γ matrices and analyzed by using both the IUSORT [10–12] and RADWARE [13] packages.

The projection spectrum from the present work is shown in Fig. 1. The nuclei principally populated in ^{16}O + ^{27}Al reaction, identified from the characteristic γ-ray transitions in the projection spectrum, were identified as ^{38}Ar, ^{41}K, and ^{41}Ca. Coincidence relations between the γ transitions were used to construct the level scheme for ^{41}Ca. The angle-dependent coincidence intensity anisotropy, deduced from the analysis of the asymmetric matrices, was used to obtain the information on the dominant multipolarity of the observed transitions, as elaborated subsequently in this section. The use of the Clover detector allowed us uniquely to obtain information on the electromagnetic nature of the transitions through linear polarization measurements, as detailed below. Furthermore, Doppler shapes and shifts were also observed in selected γ-ray-transition peaks that were analyzed for the lifetimes of the respective deexciting levels. All these measurements are expected to provide coherent and detailed information on the deduced level structure of the ^{41}Ca nucleus.

A. Spin assignment

The observed coincidence intensity anisotropy was used to infer the multipolarity of the deexciting γ transitions. The anisotropy is quantified using the R_{DCO} (directional correlations of the γ rays deexciting oriented states), defined as

$$R_{\text{DCO}} = \frac{I_{\gamma 1}(\text{at } \theta \text{ gated by } \gamma_2 \text{ at } 90^\circ)}{I_{\gamma 1}(\text{at } 90^\circ \text{ gated by } \gamma_2 \text{ at } \theta)}. \tag{1}$$

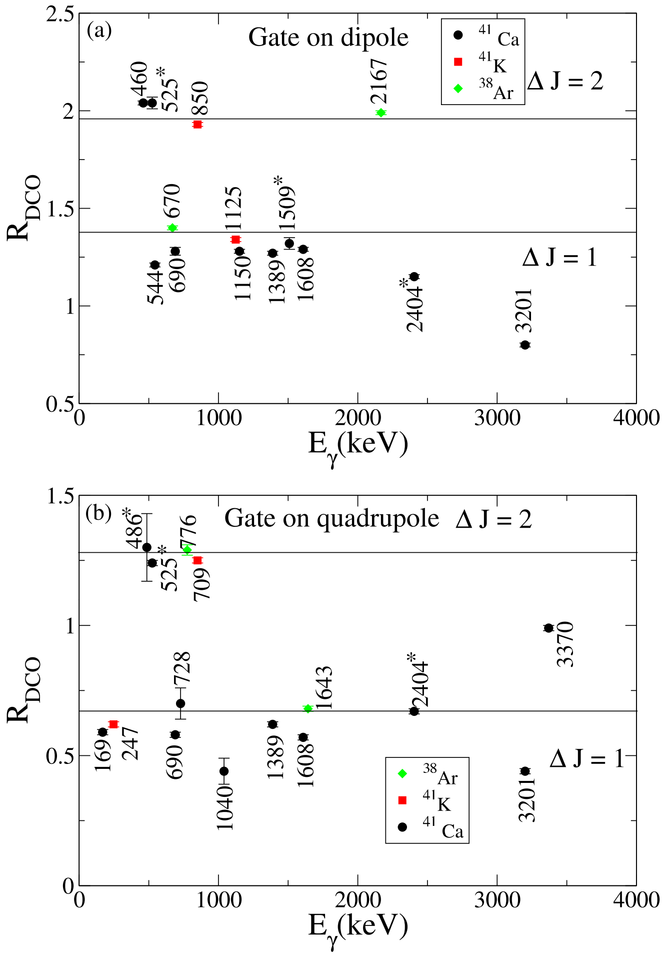

FIG. 2. Plot of R_{DCO} values for transitions in ^{38}Ar, ^{41}K, ^{41}Ca when the gate is on quadrupole and dipole transitions. New transitions in ^{41}Ca are marked by asterisks.

In the present work, the R_{DCO} was obtained from an angle-dependent asymmetric matrix with one axis representing the γ rays detected at 90° and the other axis with the coincident γ rays detected at 32°. For the present setup, if the gate were set on a pure quadrupole transition then, for a pure dipole transition, the value of R_{DCO} is $\sim$0.67 whereas, for a pure quadrupole transition, the same is $\sim$1.28. Similarly, if the gating transition is a pure dipole transition, a pure quadrupole transition would result in a R_{DCO} of $\sim$1.96, while a pure dipole would yield $R_{\mathrm{DCO}} \sim 1.37$. These values were extracted from the weighted average of the R_{DCO} values of transitions with previously known multipolarities in the ^{38}Ar and ^{41}K nuclei, populated in the same reaction. Theoretically, for the present setup, a gate on a pure quadrupole transition should result in a $R_{\mathrm{DCO}} = 1.0$ for a pure quadrupole transition and $R_{\mathrm{DCO}} = 0.4$ for a pure dipole transition. Similarly, a gate on a pure dipole transition should yield $R_{\mathrm{DCO}} = 1.0$ for a pure dipole transition and 2.1 for a pure quadrupole transition. The theoretical values have been extracted from the code ANGCOR [14].

The R_{DCO} values for the observed γ-ray transitions are presented in Fig. 2. However, this method could not be applied to the transitions that exhibited Doppler shape or shift in the angular spectrum, owing to the difficulty in applying gates on them. For such transitions (520, 775, 1586, 1752, and 4014 keV of the ^{41}Ca nucleus, for instance), the $R_{\mathrm{anisotropy}}$ value, as described in Ref. [15] was used to extract the respective multipolarity. It may be noted that, in the present setup, a pure dipole transition has $R_{\mathrm{anisotropy}} \sim 0.83$ and for a pure quadrupole $R_{\mathrm{anisotropy}} \sim 1.11$.

B. Polarization measurement

The use of Clover detectors made it possible to perform linear polarization measurements on the γ-ray transitions, which uniquely facilitated the determination of their electromagnetic nature. The linear polarization of a given γ-ray transition can be determined from the experimental asymmetry between the number of Compton scattered photons (of that transition) in a direction parallel to the reaction plane and perpendicular to it. This asymmetry is expressed as

$$\Delta_{\mathrm{pol}} = \frac{aN_{\perp} - N_{\parallel}}{aN_{\perp} + N_{\parallel}}, \tag{2}$$

where $\mathrm{N}_{\perp}$ and $\mathrm{N}_{\parallel}$ are the number of photons of a given energy scattered perpendicular to and parallel to the reaction plane, respectively. This asymmetry is determined in the Clover detectors at 90°. A set of two polarization matrices was constructed for the purpose. One of these matrices had γ-rays detected by the crystals (of the 90° Clovers) that were perpendicular to the reaction plane on one axis and coincident γ rays, detected on any other detector in the array, on the other axis. In the second matrix, the former was replaced with the γ-rays detected in the crystals parallel to the reaction plane. The factor "a" denotes the correction due to the inherent (geometric) asymmetry in the response of the Clover crystals, perpendicular and parallel to the reaction plane. This factor, defined as [16,17]

$$a = \frac{N_{\parallel}(\text{unpolarized})}{N_{\perp}(\text{unpolarized})}, \tag{3}$$

is energy dependent ($a = a_0 + a_1 E_{\gamma}$) and was measured by using a radioactive (unpolarized) source, kept at the target position. In the present work a_0 was found to be 0.99 ± 0.01, which was used in determining the polarization asymmetry. The value of a_1 was found to be very small ($\sim 10^{-6}$) and hence was not considered in the analysis.

The positive and negative value of Δ_{pol} indicate the electric and the magnetic nature of the transition, respectively, whereas a near-zero value is indicative of a mixed one. From the measured asymmetry, we can derive the polarization (P) by using

$$P = \frac{\Delta_{\mathrm{pol}}}{Q(E_{\gamma})}, \tag{4}$$

where $Q(E_{\gamma})$ [16,17] is the energy-dependent polarization sensitivity. In the present work, the value of Q has been adopted from Ref. [18].

The experimental polarization values were compared with the theoretical ones, calculated by using the procedure detailed in Refs. [19–21], and found to be in reasonable agreement, as illustrated in Fig. 3.

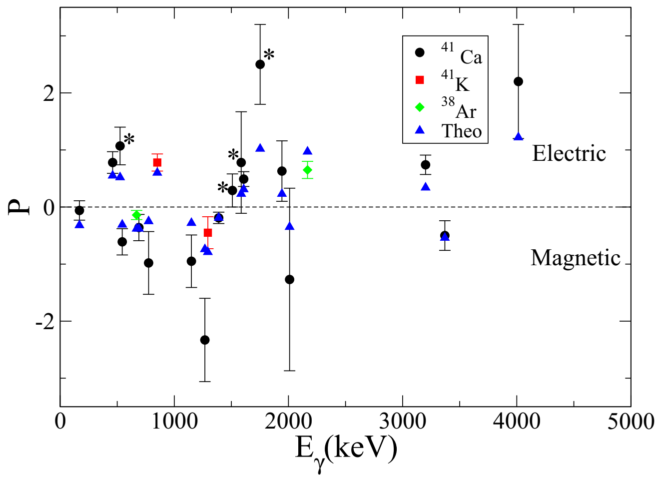

FIG. 3. Plot of experimental and calculated polarization values as a function of γ-ray energy for transitions in ^{41}Ca, ^{41}K , ^{38}Ar populated in the present experiment. The new transitions in ^{41}Ca are marked by asterisks.

These different measurements were together assimilated for construction of the proposed level scheme of the ^{41}Ca nucleus.

III. LEVEL SCHEME OF ^{41}Ca

The proposed level scheme of ^{41}Ca, following the present measurements, is illustrated in Fig. 4. Around 12 new γ-ray transitions have been observed in the present work and the level scheme of the nucleus has been extended up to an excitation energy $E_x \sim 9$ MeV and $J^\pi = 19/2^-$. Spin-parity assignments of the levels have been made based on the R_{DCO} and polarization measurements of the γ-ray transitions, described in the previous section. Some of these assignments are confirmation of the previously reported values for the earlier known levels while others are for the newly observed states in the present study. Owing to the sparse statistics, particularly at higher excitation energies, the spin-parity assignments could not be made for some of the new levels or were made tentatively. Similarly, the branching ratios could be extracted only for those transitions for which it was possible to apply a gate on top of the respective level of interest. Table I summarizes the level energies (E_x), the transition energies (E_γ) deexciting the levels along with the R_{DCO}, and Δ_{pol} and the polarization P of the transitions and the corresponding assignments, as obtained from the present work. The spin-parity assignments for some of the previously reported states could not be confirmed in the present investigation, either owing to statistics or overlap with other transitions, and have been adopted from the literature values.

Figure 5 depicts the gated spectra corresponding to the 4014 and 460 keV transitions of the ^{41}Ca nucleus. Some of the newly observed γ-ray transitions have been labeled therein. The positive- and the negative-parity states in the proposed level scheme are individually discussed hereafter.

A. Positive-parity states

The positive-parity states in ^{41}Ca have been interpreted to result from a weak coupling of the $1f_{7/2}$ neutron and the negative-parity core vibrations [2]. Most of the positive-parity levels previously reported by Lister *et al.* [2] have been observed in the present data and the spin-parity assignments are in agreement with the previous values. A few of these levels were reported to have multiple decay paths of which the most intense ones could be confirmed in the present study. For example, the 3495 keV level ($J^\pi = 5/2^+$) was reported to deexcite via the 445, 1032, 1485, and 3495 keV transitions, of which the most intense 445 and 1485 keV transitions were observed in the present experiment. Similarly, the 3974 keV level ($J^\pi = 7/2^+$) was reported to deexcite via the 3974 and 1368 keV transitions. We have not been able to confirm the presence of the 3974 keV transition from the present data, and the same is thus not included in the present level scheme.

The level at $E_x = 5219$ keV was assigned a spin and parity of $J^\pi = (17/2)^+$ by Gorodetzky *et al.* [4] and Lieb *et al.* [5], whereas the adopted J^π for this level is $(13/2)^+$, $(17/2)^+$ [22]. This level deexcites by the 1389 keV transition, which was identified as a predominantly dipole transition from the current R_{DCO} measurements ($R_{\mathrm{DCO}} = 0.62 \pm 0.01$ in the quadrupole gate and $R_{\mathrm{DCO}} = 1.26 \pm 0.01$ in the dipole gate). Furthermore, the linear polarization value ($P = -0.19 \pm 0.10$) of the transition indicates that it is a magnetic transition. The shell-model calculations, elaborated in the next section, are complied with a $J^\pi = 17/2^+$ assignment for the 5219 keV level. This assignment also conformed with the $M1$ nature of the 1389 keV ($17/2^+ \rightarrow 15/2^+$) transition, and facilitates the resolution of the ambiguity in the spin-parity value of the 5219 keV level.

The 1608 keV ($\Delta J = 1$) γ-ray transition, deexciting the level at $E_x = 6827$ keV, was assigned as $E1$, from the systematics, by Olness *et al.* [6], in spite of a negative value of the linear polarization. The current measurements have resulted in a polarization, $P = 0.49 \pm 0.13$ ($P_{\mathrm{theor}} = 0.32$), for this transition, thus confirming its electric nature. The 6827 keV level, deexciting by the 1608 keV γ, has thus been assigned $J^\pi = 19/2^-$, which is in agreement with the previous assignment by Gorodetzky *et al.* [4].

The polarization measurements of Olness *et al.* [6] for the 3370 keV transition, deexciting the 3370 keV level, resulted in $P = 60 \pm 100$ while the present investigations led to $P_{\mathrm{expt}} = -0.50 \pm 0.26$, which is in compliance with the theoretical estimate of $P_{\mathrm{theor}} = -0.54$ and indicates a dominantly magnetic character.

The new transitions, deexciting the positive-parity states in the ^{41}Ca nucleus and observed for the first time in the present work, are 242, 278, 486, 1509, and 2404 keV. Of these, the first three transitions have been found to depopulate earlier known levels of the nucleus with presumably much weaker branching than the previously reported transitions deexciting the same levels. In fact, of these three transitions, the R_{DCO} could be determined only for 486 keV, deexciting the 3370 keV level, and the results ($R_{\mathrm{DCO}} = 1.30 \pm 0.13$) comply with the $\Delta J = 2$ assignment. The 1509 and 2404 keV transitions have been found to deexcite the new levels observed

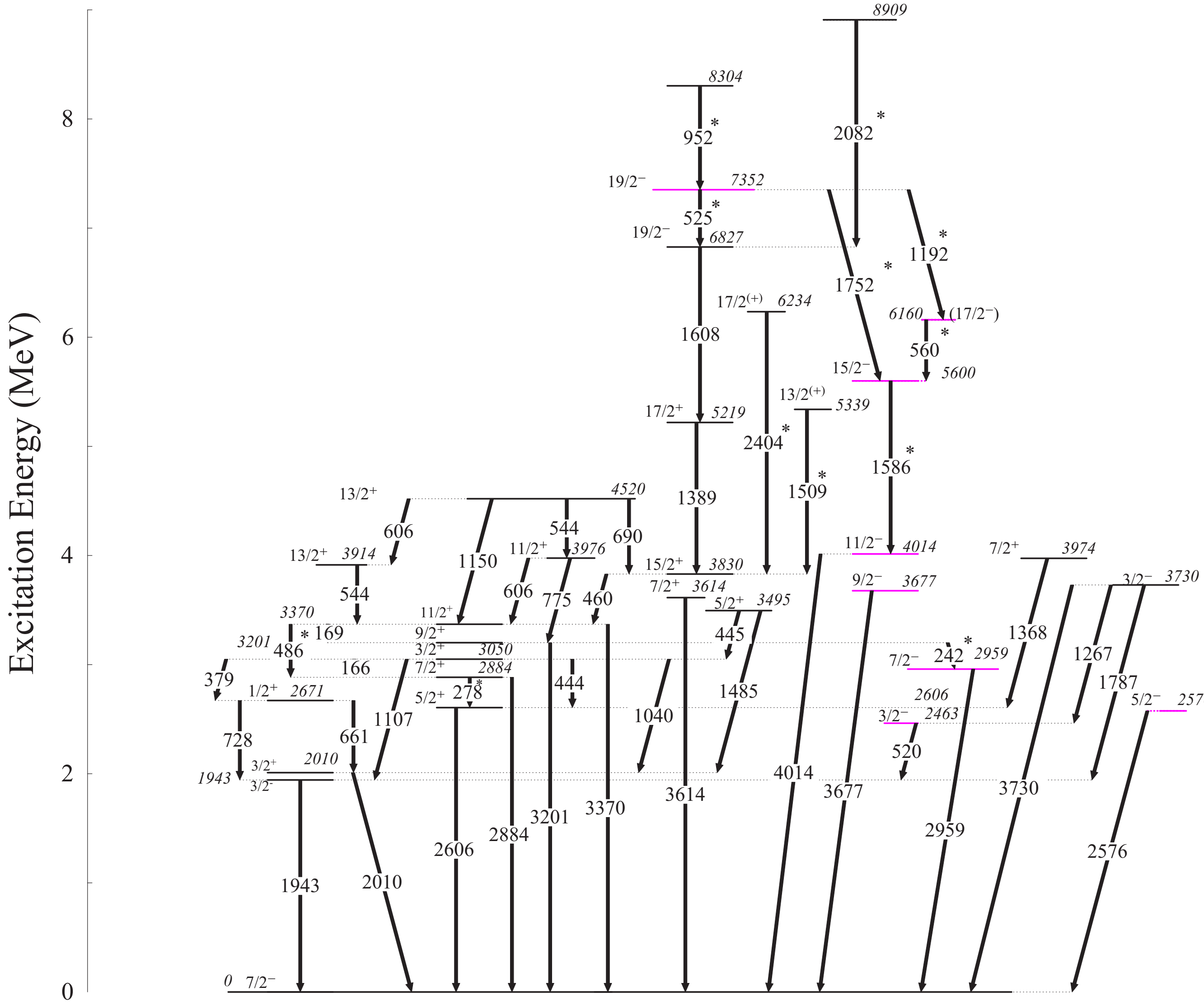

FIG. 4. Level scheme of ^{41}Ca obtained from the present work. The levels of the $K^{\pi} = 3/2^{-}$ band are marked in red.

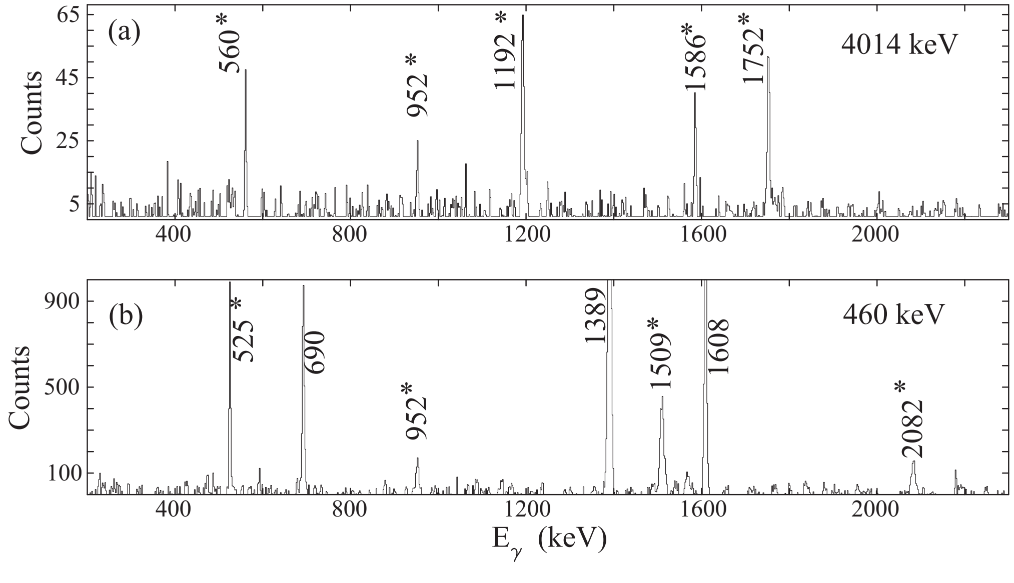

FIG. 5. Coincidence spectrum with gate on 460 and 4014 keV transitions in ^{41}Ca. The new transitions are marked by asterisks.

TABLE I. Details of γ-ray transitions in ^{41}Ca nucleus observed in the present work. Q and D superscripts in the R_{DCO} denotes quadrupole and dipole gating transitions, respectively. The A superscript denotes anisotropy, where the R_{DCO} could not be determined (see text).

E_i (keV)[a]	E_γ (keV)	E_f (keV)[a]	Br(%)	J_i^π	J_f^π	R_{DCO}	$\Delta_{(\mathrm{pol})}$	P	Multipolarity
1943	1942.6 ± 0.4	0	100	$3/2^-_1$	$7/2^-_1$	1.02 ± 0.05^{A}	0.06 ± 0.05	0.63 ± 0.53	$E2$
2010	2009.6 ± 0.3	0	100	$3/2^+_1$	$7/2^-_1$	1.65 ± 0.10^{D}	-0.12 ± 0.15	-1.27 ± 0.16	$M2 + E3$
2463	519.8 ± 0.4	1943		$3/2^-_2$	$3/2^-_1$	0.73 ± 0.04^{A}	0.05 ± 0.04	0.34 ± 0.27	$M1 + E2$
2576	2576.0 ± 1.0	0	100	$5/2^-_1$	$7/2^-_1$				$M1 + E2$[b]
2606	2605.7 ± 0.8	0	100	$5/2^+_1$	$7/2^-_1$				$E1 + M2$[b]
2671	661.4 ± 0.3	2010		$1/2^+_1$	$3/2^+_1$				$M1$
	727.6 ± 0.8	1943			$3/2^-_1$	0.70 ± 0.06^{Q}	0.56 ± 0.09	4.13 ± 0.96	$E1(+M2)$
2884	278.0 ± 1.0	2606		$7/2^+_1$	$5/2^+_1$				
	2884.0 ± 2.0	0	100		$7/2^-_1$				$E1 + M2$[b]
2959	2959.0 ± 2.0	0	100	$7/2^-_2$	$7/2^-_1$				$M1 + E2$[b]
3050	166.0 ± 1.0	2884		$3/2^+_2$	$7/2^+_1$				
	378.7 ± 1.0	2671			$1/2^+_1$				
	444.4 ± 0.5	2606			$5/2^+_1$				$M1$[b]
	1040.4 ± 0.9	2010			$3/2^+_1$	0.44 ± 0.05^{Q}			$M1$[b]
	1107.2 ± 0.7	1943			$3/2^-_1$				$E1$[b]
3201	242.0 ± 1.00	2959		$9/2^+_1$	$7/2^-_2$				
	3201.3 ± 0.3	0	100		$7/2^-_1$	0.44 ± 0.01^{Q}	0.06 ± 0.01	0.74 ± 0.17	$E1 + M2$
3370	168.8 ± 0.60	3201	69.22 ± 0.22	$11/2^+_1$	$9/2^+_1$	0.59 ± 0.01^{Q}	-0.01 ± 0.03	-0.06 ± 0.17	$M1(+E2)$
	485.7 ± 0.2	2884	0.29 ± 0.05		$7/2^+_1$	1.30 ± 0.13^{Q}			
	3369.8 ± 0.4	0	30.57 ± 0.06		$7/2^-_1$	0.99 ± 0.01^{Q}	-0.04 ± 0.02	-0.50 ± 0.26	$M2 + E3$
3495	445.3 ± 0.5	3050		$5/2^+_2$	$3/2^+_2$				
	1484.7 ± 0.7	2010			$3/2^+_1$				$M1 + E2$[b]
3614	3614.0 ± 2.0	0	100	$7/2^+_2$	$7/2^-_1$				$E1 + M2$[b]
3677	3677.0 ± 2.0	0	100	$9/2^-_1$	$7/2^-_1$				$M1 + E2$[b]
3730	1267.3 ± 0.8	2463		$3/2^-_3$	$3/2^-_2$		-0.26 ± 0.07	-2.33 ± 0.73	$M1 + E2$[b]
	1786.8 ± 0.5	1943			$3/2^-_1$				$M1 + E2$[b]
	3730.0 ± 1.0	0	100		$7/2^-_1$				$E2$[b]
3830	460.3 ± 0.3	3370	100	$15/2^+_1$	$11/2^+_1$	2.04 ± 0.01^{D}	0.12 ± 0.02	0.78 ± 0.19	$E2$
3914	544.2 ± 0.6	3370	100	$13/2^+_1$	$11/2^+_1$	1.21 ± 0.01^{D}	-0.09 ± 0.03	-0.61 ± 0.23	$M1(+E2)$
3974	1368.2 ± 0.3	2606		$7/2^+_3$	$5/2^+_1$				$M1 + E2$[b]
3976	606.0 ± 1.0	3370		$11/2^+_2$	$11/2^+_1$				
	775.2 ± 0.6	3201			$9/2^+_1$	0.79 ± 0.03^{A}	-0.13 ± 0.07	-0.98 ± 0.55	$M1 + E2$
4014	4014.0 ± 2.00	0	100	$11/2^-_1$	$7/2^-_1$	1.10 ± 0.05^{A}	0.17 ± 0.07	2.2 ± 1.0	$E2$
4520	544.3 ± 0.7	3976		$13/2^+_2$	$11/2^+_2$				$M1 + E2$
	606.0 ± 1.0	3914			$13/2^+_1$				
	690.4 ± 0.5	3830			$15/2^+_1$	0.58 ± 0.01^{Q}	-0.05 ± 0.03	-0.36 ± 0.23	$M1 + E2$
	1150.2 ± 0.8	3370			$11/2^+_1$	1.28 ± 0.01^{D}	-0.11 ± 0.05	-0.95 ± 0.46	$M1 + E2$
5219	1389.4 ± 0.3	3830	100	$17/2^+_1$	$15/2^+_1$	0.62 ± 0.01^{Q}	-0.02 ± 0.01	-0.19 ± 0.10	$M1(+E2)$
5339	1508.8 ± 0.6	3830	100	$13/2^{(+)}_3$	$15/2^+_1$	1.32 ± 0.03^{D}	0.03 ± 0.03	0.29 ± 0.29	$M1 + E2$
5600	1586.0 ± 2.0	4014	100	$15/2^-_1$	$11/2^-_1$	1.68 ± 0.62^{A}	0.08 ± 0.09	0.78 ± 0.89	$E2$
6160	560.0 ± 0.2	5600	100	$(17/2^-_1)$	$15/2^-_1$				
6234	2404.4 ± 0.7	3830	100	$17/2^{(+)}_2$	$15/2^+_1$	0.67 ± 0.01^{Q}			
6827	1607.6 ± 0.9	5219	100	$19/2^-_1$	$17/2^+_1$	0.57 ± 0.01^{Q}	0.05 ± 0.01	0.49 ± 0.13	$E1$
7352	524.8 ± 0.3	6827		$19/2^-_2$	$19/2^-_1$	1.24 ± 0.01^{Q}	0.16 ± 0.04	1.07 ± 0.33	$E2$
	1192.3 ± 0.3	6160			$17/2^-_1$				
	1752.0 ± 2.0	5600			$15/2^-_1$	1.36 ± 0.06^{A}	0.25 ± 0.06	2.5 ± 0.70	$E2$
8304	951.7 ± 0.6	7352	100						
8909	2082.2 ± 0.8	6827	100						

[a] The quoted energies are within ±2 keV.

[b] From NNDC.

in the present measurements: 5339 and 6234 keV, respectively. From the R_{DCO} measurements, these transitions have been identified as predominantly dipole transitions. However, the polarization measurements could be carried out only for the 1509 keV transition, albeit with high uncertainty, following which the 5339 keV level has been assigned $J^\pi = 13/2^{(+)}$. The 6234 keV state, deexcited by the 2404 keV transition, has been assigned a spin of $17/2^{(+)}$, following the dipole character of the latter and its parity is unknown from the present measurements. The positive-parity assignment for the 5339 and 6234 keV levels has been tentatively made from comparison with the shell-model calculations (cf. Fig. 7).

B. Negative-parity states

The negative-parity states in ^{41}Ca may originate from excitation of the valence neutron from the $f_{7/2}$ ground state to the $p_{3/2}$, $p_{1/2}$, and $f_{5/2}$ orbitals [2]. The previously reported negative-parity states at 1943 ($J^\pi = 3/2^-_1$), 2463 ($J^\pi = 3/2^-_2$), 2959 ($J^\pi = 7/2^-_2$), 3677 ($J^\pi = 9/2^-_1$), 3730 ($J^\pi = 3/2^-_3$), and 4014 ($J^\pi = 11/2^-_1$) keV have been confirmed in the present experiment along with their respective spin-parity assignments. The 2576 keV γ transition, deexciting the 2576 keV level, could not be confirmed from the present data due to overlapping transitions from the other nuclei populated in the same reaction and has been adopted from the earlier measurements. The 3677 keV level was reported to deexcite by the 718 and the 3677 keV transitions, of which the 718 keV transition, with a reported branching of ~6%, could not be observed in the present work. Similarly, for the 3730 keV level reported to be deexcited by the 1154, 1267, 1787, and 3730 keV transitions, the 1154 keV transition could not be observed in this data.

The negative-parity states in the ^{41}Ca nucleus have previously been interpreted beyond the simple single-particle excitations and have been attributed to the interaction of the single-particle states to the excitations of the core. Lister *et al.* [2] proposed that the states $3/2_2{}^-$ to $11/2_1{}^-$ are members of a deformed $K^\pi = 3/2^-$ band originating from the excitations of four particles to the $1/2^-[330]$ Nilsson level leaving behind four holes in the $3/2^+[202]$ state along with the odd neutron in the $3/2^-[321]$ level. Following the present measurements, three new levels at $E_x = 5600$, 6160, and 7352 keV, with $J^\pi = 15/2^-$, $17/2^-$, $19/2^-$, have been identified as higher-spin members of the aforementioned $K^\pi = 3/2^-$ band. The intraband 1586 keV ($15/2^- \rightarrow 11/2^-$) transition, deexciting the 5600 keV level, has been established as an $E2$ transition from the present anisotropy (1.68 ± 0.62) and polarization (0.78 ± 0.89) measurements. Similarly, the 1752 keV ($19/2^- \rightarrow 17/2^-$) intraband transition, with anisotropy 1.36 ± 0.06 and polarization 2.5 ± 0.70, has also been identified to be of $E2$ character in the present study. The 560 keV transition, deexciting the 6160 keV state, could not be analyzed for the multipolarity and the electromagnetic nature, although the level has been attributed to the deformed band from the systematics discussed in the next section.

The limited statistics for the 952 and 2082 keV transitions, in the higher-spin domain, did not allow for their R_{DCO}, anisotropy, or polarization measurements.

C. Lifetime analysis

Level lifetimes are crucial because they provide unique indicators to the underlying microscopic configurations of the observed structure. The observation of Doppler shifts and shapes allowed for determination of the level lifetimes from the Doppler shift attenuation method (DSAM) by using the LINESHAPE [23] code.

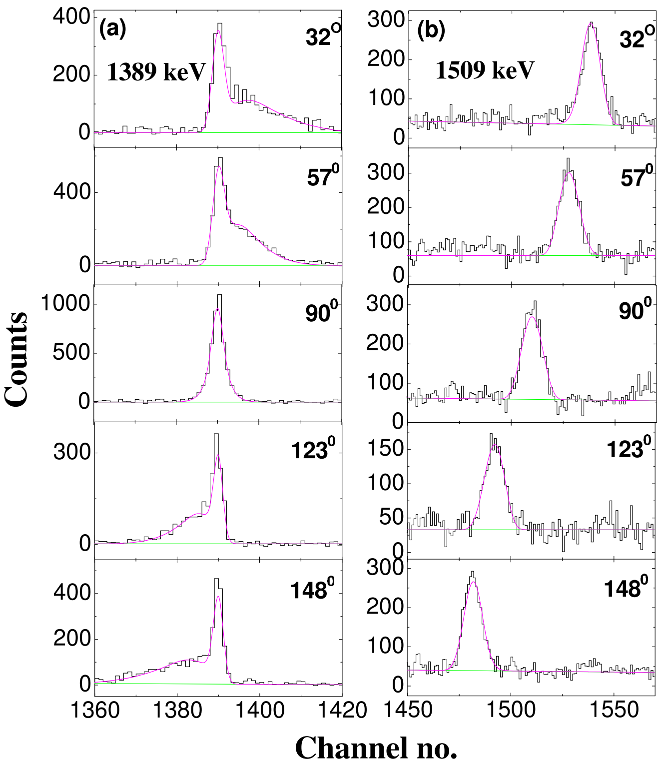

FIG. 6. Representative fit of Doppler shape for 1389 and 1509 keV γ rays in ^{41}Ca.

The conventional DSAM measurement employ a "thin" target followed by a thick, high-Z backing. In the present case, however, the target and the backing were both of Al. The statistical model calculations indicated that the production of ^{41}Ca in the reaction ^{27}Al(^{16}O ,np) was possible up to an incident beam energy of 26 MeV. Given that the primary beam energy in this experiment was 34 MeV, this implies that

TABLE II. Lifetimes of the states in ^{41}Ca from the present work (labeled I) in comparison to the previously reported values from NNDC [22] (labeled II). The quoted uncertainties include the effects of the uncertainties in the stopping powers.

J_i^π	E_x (keV)	E_γ (keV)	τ (fs) I	τ (fs) II
$13/2^+_1$	3914	544	1650^{+90}_{-160}	2090^{+380}_{-380}
$13/2^+_2$	4520	690	<241[a]	<71
		606	<248[a]	
$17/2^+_1$	5219	1389	47^{+23}_{-7}	<40
$(13/2^+_3)$	5339[b]	1509	<71[a]	
$(17/2^+_2)$	6234[b]	2404	<183[a]	
$19/2^-_1$	6827	1608	1640^{+100}_{-100}	<2450
$(19/2^-_2)$	7352[b]	525	716^{+157}_{-102}	

[a] The presence of a dominant side feeding allowed for assignment of only an upper limit on the lifetime.

[b] New level from our present work.

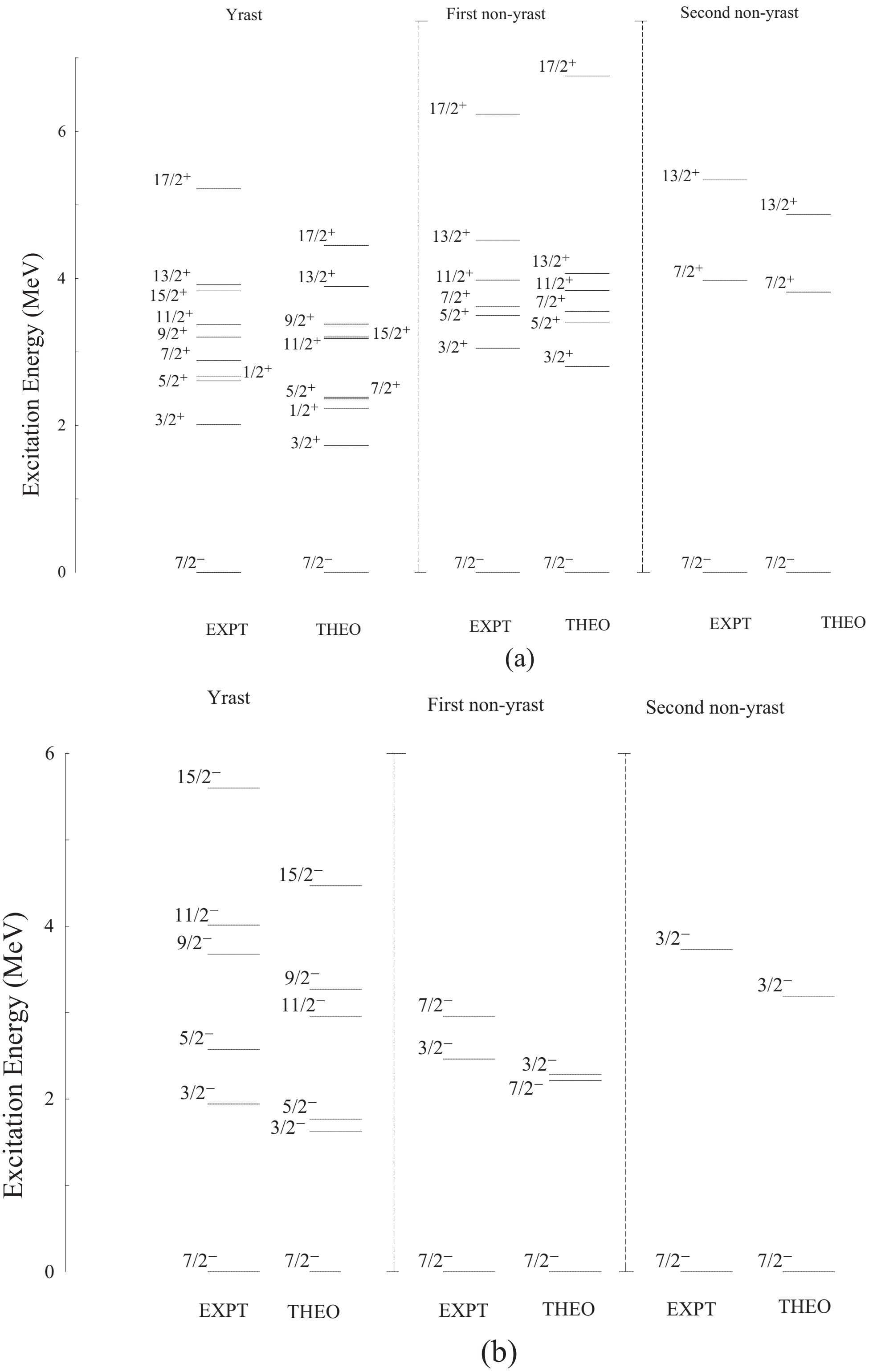

FIG. 7. Comparison of experimental and shell-model calculated level energies in ^{41}Ca.

an Al thickness corresponding to the energy loss of 8 MeV (i.e., 34 MeV − 26 MeV) of the ^{16}O beam would contribute to the production of ^{41}Ca. The corresponding Al thickness was calculated by using the SRIM code to be 1.6 mg/cm^2. It may be noted that, within this thickness, the beam continuously looses energy and, consequently, the cross section of production of ^{41}Ca changes. This evolving cross section was taken into account for simulation of the slowing down process of the recoil in the target and the backing media (both Al, in this case) by using a modified version of the DECHIST code within

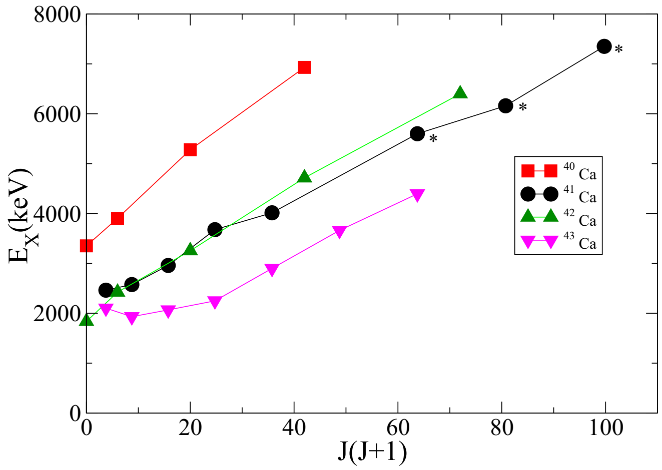

FIG. 8. Plot of excitation energy against $J(J+1)$ for negative-parity states in ^{41}Ca. The $K^{\pi} = 0^{+}$ deformed bands in ^{40,42}Ca and the $K^{\pi} = 3/2^{-}$ bands in ^{43}Ca are also shown for comparison. New levels in ^{41}Ca are marked by asterisks.

the LINESHAPE package. The modification also included use of updated and experimentally benchmarked stopping powers from the SRIM program [24]. The subsequent steps in the Doppler shape analysis were carried out by following the conventional methodology as outlined in Ref. [24].

The major source of uncertainty in these calculations originates from the corresponding uncertainty in determination of the stopping powers, which are typically ±10%, in conservative limits, and the resulting dispersion in the level lifetimes have been included in the quoted uncertainties. The fitting uncertainties, which were estimated following the χ^2 analysis, have also been included.

Figure 6 shows a representative fit of Doppler shape for 1389 and 1509 keV γ transition deexciting from 5219 and 5339 keV levels, respectively, in ^{41}Ca. The level lifetime of the 5219 keV level was reported as $\leqslant$40 fs [22] and the obtained value is 47^{+23}_{-7} fs. Lifetime of the several other known levels in the ^{41}Ca nucleus were determined and found in good agreement with the values reported previously. The level lifetimes for three levels have been estimated for the first time, two of these being effective lifetimes due to absence of any top feeding transitions. The results are summarized in Table II.

The members of the extended deformed band ($E_{\gamma} = 560$, 1586, 1752, and 4014 keV), exhibit a Doppler shape or shift and might have been useful for probing the characteristics of the deformed structure. However, owing to the sparse statistics, these transitions could not be analyzed for the level lifetimes in the present endeavor and might be taken up for a subsequent measurement.

IV. SHELL-MODEL CALCULATIONS

Large-basis shell-model calculations have been used to interpret the observed level structure of the ^{41}Ca nucleus, following the present work. The calculations were carried out by using the NUSHELLX@MSU code [25]. The chosen model space consisted of $1d_{3/2}$, $2s_{1/2}$, $1f_{7/2}$, and $2p_{3/2}$ orbitals outside the ^{28}Si core and the interaction used was ZBM2 [26].

Figure 7 presents the comparison between the experimental and predicted excitation energies and, as is evident from the figure, the two are in reasonable agreement. However, one does observe discrepancies between the two, especially at higher energies. A possible reason could be the omission of dominant configurations arising from excitation of nucleons from the $d_{5/2}$ orbital, which could not be included in the calculations owing to the computational limitations. It is observed that the model calculations poorly reproduce the level energies of the $K^{\pi} = 3/2^{-}$ deformed band, consisting of the $J^{\pi} = 3/2^{-}_{2}$, $5/2^{-}_{1}$, $7/2^{-}_{2}$, $9/2^{-}_{1}$, and $11/2^{-}_{1}$ states, probably owing to the restricted model space. These members of the deformed band in ^{41}Ca, including the new levels following the present measurements, have been represented in a plot of $J(J+1)$ versus excitation energies shown in Fig. 8; the plot also includes members of the $K^{\pi} = 0$, $3/2^{-}$ bands in the neighboring isotopes of Ca [2]. As is evident from the Fig. 8, the qualitative trend exhibited by the established deformed bands in this region holds good for the extended $K^{\pi} = 3/2^{-}$ band in ^{41}Ca. This is indicative of the persistence of deformation up to the highest observed spin of $J^{\pi} = 19/2^{-}$.

The transition probabilities from the levels whose lifetimes could be determined in the present work were also calculated using the shell model and the results are presented in Table III and show reasonable agreement with the experimental values.

TABLE III. Comparison of the experimental transition probabilities and branching ratios,wherever possible, with those from the shell-model calculations. Mixing ratios for calculation of the $B(M1)$ and $B(E2)$ values are from the shell-model calculations, unless noted otherwise.

E_x	E_{γ}	M	δ	Expt.			SM		
				$B(M1)$ (μ_n^2)	$B(E2)$ (e^2 fm^4)	Br	$B(M1)$ (μ_n^2)	$B(E2)$ (e^2 fm^4)	Br
3914	544	$M1 + E2$[a]	-0.01	$0.214^{+0.023}_{-0.011}$	$1.037^{+0.113}_{-0.053}$	1.00[b]	0.344	2.78	0.35
4520	690	$M1 + E2$	-0.11	>0.206	>75.06	0.29[c]	0.136	4.66	0.08
5219	1389	$M1 + E2$[a]	0.03	$0.450^{+0.079}_{-0.147}$	$3.02^{+0.530}_{-0.99}$	1.00[b]	0.262	0.838	0.99
5339	1509	$M1 + E2$	0.03	>0.233	>1.32	1.00[b]	0.110	0.525	0.40
6234	2404	$(M1 + E2)$	6.43	>0.0005	>54.2	1.00[b]	0.0009	4.54	0.37

[a] Mixing ratio from NNDC.

[b] Present work.

[c] From NNDC.

It can be generally stated that the limited success of the shell-model calculations in representing the level structure of the ^{41}Ca nucleus indicates the requirement for a larger basis space so as to include the 3p-2h, 5p-4h excitations and an interaction that allows for the same.

V. CONCLUSION

The present study has extended the level structure of the ^{41}Ca nucleus, up to an excitation energy of $E_x \sim 9$ MeV and spin $J^\pi = 19/2^-$, with the observations of about 12 new γ-ray transitions. The $K^\pi = 3/2^-$ deformed band has also been extended to higher $(19/2^-)$ spins and established to follow the same trend as the lower-spin members in the excitation energy versus $J(J+1)$ plot. The characteristics of the band have been compared with similar structures observed in the neighboring Ca isotopes and have been found to be in overlap. Level lifetimes using DSAM were also extracted from the Doppler shapes or shifts observed on certain transition peaks.

Large-basis shell-model calculations, using ^{28}Si core and $1d_{3/2}$, $2s_{1/2}$, $1f_{7/2}$, and $2p_{3/2}$ orbitals as the basis, were carried out for the level energies and the transition probabilities in the ^{41}Ca nucleus. The agreement with the experimental results, however, was found to be only a modest. The limited success of these calculations indicated the need for a larger basis space so as to incorporate multiparticle-multihole configurations for better overlap with the data.

ACKNOWLEDGMENTS

The authors thank all the participants of the INGA collaboration for their help in setting up the facility at IUAC, New Delhi. We thank the Pelletron staff at IUAC, New Delhi for their excellent support during the experiment. Discussions with Prof. Brown and Prof. Gautam Gangopadhyay on the shell-model calculations have been of much help and are deeply appreciated. Thanks are due to Kausik Basu of UGC-DAE CSR, Kolkata Centre, and Dr. B.K. Yogi of Government College Kota for their help during the experiment. This work has been supported in part by the Department of Science and Technology, Government of India (Grant No. IR/S2/PF-03/2003-III) and the U.S. National Science Foundation (Grants No. PHY07-58100 and No. PHY-1419765).

---

[1] J. Styczen, J. Chevallier, B. Haas, H. Schulz, P. Taras, and M. Toulemonde, Nucl. Phys. A **262**, 317 (1976).

[2] C. J. Lister, A. M. Al-Naser, A. H. Behbehani, L. L. Green, P. J. Nolan, and J. F. Sharpey-Schafer, J. Phys. G: Nucl. Phys. **6**, 619 (1980).

[3] C. J. Lister, A. J. Brown, L. L. Green, A. N. James, P. J. Nolan, and J. F. Sharpey-Schafer, J. Phys. G: Nucl. Phys. **2**, 577 (1976).

[4] P. Gorodetzky, J. J. Kolata, J. W. Olness, A. R. Poletti, and E. K. Warburton, Phys. Rev. Lett. **31**, 1067 (1973).

[5] K. P. Lieb, M. Uhrmacher, J. Dauk, and A. M. Kleinfeld, Nucl. Phys. A **223**, 445 (1974).

[6] J. W. Olness, A. H. Lumpkin, J. J. Kolata, E. K. Warburton, J. S. Kim, and Y. K. Lee, Phys. Rev. C **11**, 110 (1975).

[7] S. Muralithar, K. Rani, R. Kumar, R. P. Singh, J. J. Das, J. Gehlot, K. S. Golda, A. Jhingan, N. Madhavan, S. Nath *et al.*, Nucl. Instrum. Methods Phys. Res., Sect. A **622**, 281 (2010).

[8] S. Venkataramanan, A. Gupta, K. Rani, R. P. Singh, S. Muralithar, B. P. A. Kumar, and R. K. Bhowmik, Proc. DAE Symp. Nucl. Phys. **45B**, 420 (2002).

[9] B. P. A. Kumar, E. T. Subramanium, K. M. Jayan, S. Mukherjee, and R. K. Bhowmik, in *Proceedings on the Symposium on Advances in Nuclear and Allied Instruments, India* (Tata McGraw-Hill, New Delhi, 1997), p. 51.

[10] N. S. Pattabiraman, S. N. Chintalapudi, and S. S. Ghugre, Nucl. Instrum. Methods Phys. Res., Sect. A **526**, 432 (2004).

[11] N. S. Pattabiraman, S. N. Chintalapudi, and S. S. Ghugre, Nucl. Instrum. Methods Phys. Res., Sect. A **526**, 439 (2004).

[12] N. S. Pattabiraman, S. S. Ghugre, S. K. Basu, U. Garg, S. Ray, A. K. Sinha, and S. Zhu, Nucl. Instrum. Methods Phys. Res., Sect. A **562**, 222 (2006).

[13] D. C. Radford, Nucl. Instrum. Methods Phys. Res., Sect. A **361**, 297 (1995).

[14] E. S. Macias, W. D. Ruhter, D. C. Camp, and R. G. Lanier, Comput. Phys. Commun. **45B**, 75 (1976).

[15] R. Chakrabarti, S. Mukhopadhyay, R. Bhattacharjee, S. S. Ghugre, A. K. Sinha, A. Dhal, L. Chaturvedi, M. K. Raju, N. Madhavan, R. P. Singh *et al.*, Phys. Rev. C **84**, 054325 (2011).

[16] K. Starosta, Nucl. Instrum. Methods Phys. Res., Sect. A **423**, 16 (1999).

[17] P. M. Jones, L. Wei, F. A. Beck, P. A. Butler, T. Byrski, G. Duchene, G. de France, G. D. J. F. Hannachi, and B. Kharraja, Nucl. Instrum. Methods Phys. Res., Sect. A **362**, 556 (1995).

[18] S. S. Bhattacharjee, R. Bhattacharjee, R. Chakrabarti, R. Raut, S. S. Ghugre, A. K. Sinha, T. Trivedi, L. Chaturvedi, S. Saha, J. Sethi *et al.*, Phys. Rev. C **89**, 024324 (2014).

[19] T. Aoki, K. Furuno, Y. Tagishi, S. Ohya, and J. Ruan, At. Data Nucl. Data Tables **23**, 349 (1979).

[20] E. D. Mateosian and A. W. Sunyar, At. Data Nucl. Data Tables **13**, 391 (1974).

[21] T. Yamazaki, Nucl. Data, Sect. A **3**, 1 (1967).

[22] www.nndc.bnl.gov.

[23] J. C. Wells and N. R. Johnson, ORNL Rep. **6689**, 44 (1991).

[24] R. Bhattacharjee, S. S. Bhattacharjee, K. Basu, P. V. Rajesh, R. Raut, S. S. Ghugre, D. Das, A. K. Sinha, L. Chaturvedi, U. Garg, S. Ray, B. K. Yogi, M. K. Raju, R. Chakrabarti, S. Mukhopadhyay, A. Dhal, R. P. Singh, N. Madhavan, and S. Muralithar, Phys. Rev. C **90**, 044319 (2014).

[25] W. A. Richter and B. A. Brown, Phys. Rev. C **80**, 034301 (2009).

[26] E. Caurier, K. Langanke, G. Martínez-Pinedo, F. Nowacki, and P. Vogel, Phys. Lett. B **522**, 240 (2001).